Nonlinear Waves.
Solitons. Autowaves. Self-Organization

Izvestiya Vysshikh Uchebnykh Zavedeniy. Applied Nonlinear Dynamics. 2022;30(1)

Article
DOI: 10.18500/0869-6632-2022-30-1-109-124

Selection of spatial modes in an ensemble of non-locally coupled chaotic maps

A. V. Shabunin

Saratov State University, Russia
E-mail: ✉shabuninav@info.sgu.ru
Received 14.08.2021, accepted 05.10.2021, published 31.01.2022

Abstract. *Purpose* of this work is to determine regularities of formation of spatial structures in an ensemble of chaotic systems with non-local diffusion couplings and to study how these structures depend on the wave response of the digital filter formed by the ensemble couplings structure. *Methods.* The study was carried out by numerical simulation of an ensemble of logistic maps, calculation of its typical oscillatory regimes and their spectral analysis. The network was considered as a digital filter with a frequency response depending on the coupling parameters. Correlation between the spatial spectra and the amplitude-frequency response of the coupling filter and the mutual coherence of oscillations when the coupling parameters change were considered. *Results.* The system of couplings between chaotic maps behaves like a wave filter with selective properties, allowing spatial modes with certain wavelengths to exist and suppressing others. The selection of spatial modes is based on the wave characteristic of the coupling filter, the type of which is determined by the radius and the magnitude of couplings. At strong coupling the wave characteristics for ensembles with local and non-local couplings are qualitatively different, therefore they demonstrate essencially different behavior. *Discussion.* Using spectral methods for dynamics analysis systems with complex network topologies seems to be a promising approach, especially for research of synchronization and multistability in ensembles of chaotic oscillators and maps. The found regularities generalize the results known for ensembles of maps with local couplings. They also can be applied to ensembles of self-sustained oscillators.

Keywords: spatiotemporal chaos, ensembles of maps, synchronization, spatial filtering.

Acknowledgements. This work was supported by Russian Foundation for Basic Research and DFG, grant No 20-52-12004.

For citation: Shabunin AV. Selection of spatial modes in an ensemble of non-locally coupled chaotic maps. Izvestiya VUZ. Applied Nonlinear Dynamics. 2022;30(1):109–124. DOI: 10.18500/0869-6632-2022-30-1-109-124

Introduction

Ensembles of oscillatory systems are of considerable interest for physics and other natural sciences. They serve as models of spatially distributed environments and make it possible to identify mechanisms of phenomena of cooperation, competition and self-organization. Of particular

interest are ensembles of oscillators with chaotic behavior [1, 2]. A wide range of phenomena is observed in such systems. For example: synchronization of chaotic oscillations [2–6], traveling waves [7, 8], formation of dissipative spatial structures [9–11], developed multistability [12–17].

In recent years, along with the study of ensembles with local connections between nodes, networks with more complex topology have attracted considerable interest. One example of such networks can be considered systems with *long-range connections* (DS), when not only the nearest neighbors interact, but also elements that are distant from each other the ensemble. Interest in ensembles with DS is fueled by the development of modern infocommunication technologies, as well as research in biology, neurophysiology and sociology. Interest in the dynamics of ensembles with DS, it is also manifested in connection with the discovery of a special type of cluster structures in them, called *chimeras* [18–22].

High-dimensional systems demonstrate a wide variety coexisting modes. Therefore, they are difficult to analyze by bifurcation analysis methods, which are used for simpler systems. In such cases, it is convenient to use integral characteristics. They allow predicting the typical behavior of an ensemble under standard initial conditions. For example, spectral analysis based on the calculation of temporal and spatial spectra. The transition from a time description to a frequency description is traditional for both physics and engineering. It allows you to diagnose synchronization between oscillators of the ensemble and quantify its magnitude [23]. For some types of coupling (for example, diffusion), the use of the spectral method makes it possible to determine the conditions for synchronizing chaotic oscillations in an ensemble depending on the magnitude of the bonds [6].

In this study, we propose to consider the connections between the oscillators of the network as a spatial digital filter. Its properties are characterized by a wave characteristic. Previously, the digital filter method was used to analyze the patterns of formation of multistability of periodic orbits in an ensemble of maps with long-range connections [24] and to analyze spatial modes in an ensemble with local diffusion connections [25]. In this study, we consider the selection of spatial modes in an ensemble with non-local connections, which is in the mode of space-time chaos. Such a regime combines many metastable space-time states in its composition and its properties depend on the connections between the elements of the ensemble.

1. Spatial selection in ensembles with long-range communication

Consider an ensemble of N maps with symmetric connection, closed in a ring

$$x_i(n+1) = F\left(x_i(n)\right) + \frac{\gamma}{2L}\sum_{j=-L}^{L}\left[F\left(x_{i+j}(n)\right) - F\left(x_i(n)\right)\right]. \tag{1}$$

Here $x_i(n)$ is a dynamic variable depending on the discrete time n and the spatial coordinate i given on the segment $[1:N]$; $F(x)$ — a function defining the dynamics of a single mapping; γ — the strength of connections between the elements of the ensemble, $L = 1, 2, ..., N/2$ — their maximum range (radius of connections). Due to the ring topology of the network, all operations with lower indexes are performed modulo N.

The network communication system (1) is a linear filter with selective properties. To verify this, we rewrite the equation (1) as

$$x_i(n+1) = \sum_{j=-L}^{L} h_j F\left(x_{i+j}(n)\right), \tag{2}$$

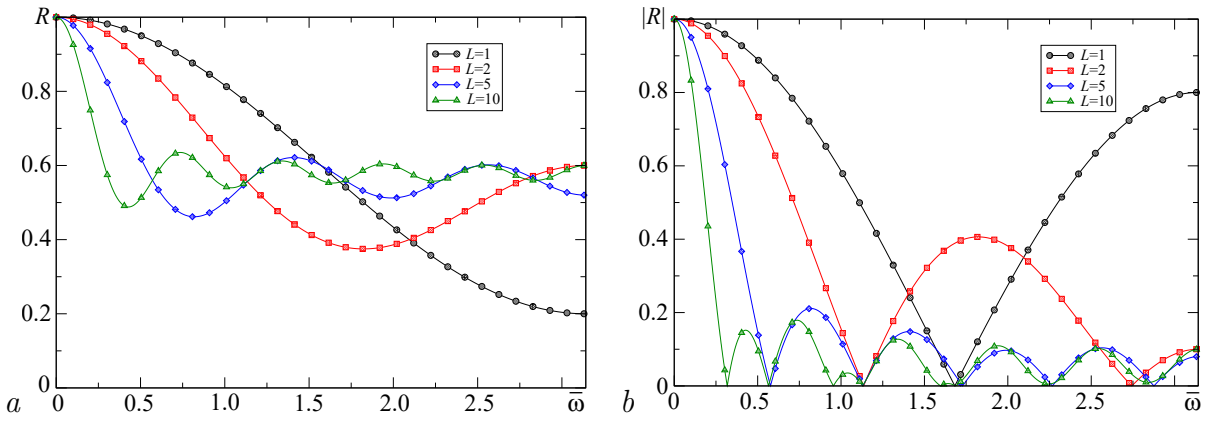

Fig. 1. Plots of the frequency response of the coupling filter at $\gamma = 0.4$ (a) and its amplitude-frequency response at $\gamma = 0.9$ (b)

where $h_0 = 1 - \gamma$, $h_j = \gamma/(2L)$ $(j = \pm 1, ..., \pm L)$ — positive constants. The formula (2) can be represented as a superposition of a nonlinear mapping

$$y_i(n) = F\left(x_i(n)\right)$$

and linear convolution by spatial coordinate

$$x_i(n+1) = \sum_{j=-L}^{L} h_j y_{i+j}\left(n\right).$$

The last equation coincides in form with the equation of a linear digital filter with the impulse response $\mathbf{h}$ acting on the spatial trajectory $\mathbf{y}$. The frequency (wave) characteristic of such a filter is the Fourier transform of its impulse response; for the above values of the coefficients h_j it will take the form:

$$R(\bar{\omega}) = 1 - \gamma + \frac{\gamma}{L} \sum_{l=1}^{L} \cos\left(l\bar{\omega}\right). \tag{3}$$

Here R — filter transfer coefficient, $\bar{\omega} \in [0 : \pi]$ — normalized spatial frequency (wave number)[1].

Consider the properties of R defined by the formula (3). $R(\bar{\omega})$ is a real quantity, which is a consequence of the symmetry of the connections in the ensemble[2]. The graph of the function $R(\bar{\omega})$ is determined by the radius of the connections and for the values of $L = 1$, 2, 5, 10, which are considered in this study, it is presented in Fig. 1, *a*. It is clearly seen that for $L > 1$, the transmission coefficient has a *lobe* structure with a pronounced maximum in the vicinity of zero (*main lobe*) and oscillating "tails" (*side lobes*) on the periphery. This form resembles the well-known in radio engineering function sinc. This similarity is not accidental, since the expression for R is a discrete analogue of the expression for the spectrum of a rectangular pulse, and for large L the ratio (3) is well approximated by the formula

$$R(\bar{\omega}) \simeq 1 - \gamma + \gamma\,\mathrm{sinc}\left((L + 0.5)\bar{\omega}\right). \tag{4}$$

"Tails" of the frequency response are raised above the abscissa axis by some constant value ΔR, which at $L \gg 1$ is close to the value $1 - \gamma$. Therefore, the value of the bond strength determines

[1]To distinguish spatial frequencies from the usual ones, we will mark them with a dash from above.

[2]For ensembles with asymmetric connections, R will be complex.

the intensity of the selective properties of the filter. Significantly affects the shape $R(\bar{\omega})$ also the radius of the links. With an increase in L, the number of side lobes increases, and their width decreases (at $L \gg 1$, the width of the lobes is the inverse of the radius of the connections). Thus, in the range of coupling values $0 < \gamma \leqslant 1$, the main lobe is always raised above the side ones, the smaller the value, the higher their number. With weak coupling, the filter is transparent for any wavelengths; at the same time, with increasing coupling, the selective properties are enhanced towards suppression of short-wave modes.

From the expression (3) it is easy to obtain the phase-frequency (RF) and amplitude-frequency (AFC) characteristics of the coupling filter.

Phase frequency response. Since the transmission coefficient is a real number, the phase shift of the spatial filter $\phi = \arg(R)$ is either zero for positive R, or π for negative. Thus, the frequency response is either a constant or a piecewise constant function of the wave number $\bar{\omega}$. The latter case is implemented if the communication parameter exceeds some critical value

$$\gamma_c = \frac{2}{4 - \arctan(L-1)}. \tag{5}$$

Amplitude-frequency response. Type of amplitude-frequency response $A(\bar{\omega}) = |R(\bar{\omega})|$ will also be different for $\gamma < \gamma_c$ and $\gamma > \gamma_c$. In the first case, the frequency response coincides with the corresponding graph $R(\bar{\omega})$, shown in Fig. 1, *a*. Since the maximum value of the transmission coefficient is reached at zero frequency, the frequency response form will correspond to the low-pass filter (LPF); in this case, the main lobe can be considered *bandwidth*, and the side lobes — *barrier band* of the filter. With the growth of γ, the average level of the barrier band decreases, the selective properties of the filter are enhanced. At $\gamma > \gamma_c$, the frequency response form becomes more complex. This can be seen by the example of the graphs in Fig. 1, *b*, but at $L > 1$ it continues to correspond to the LPF. An exception is the case of local connections, in which the transition of γ through a critical value leads to a change in the type of filter from low frequency to blocking (see [25]).

Thus, a system of symmetric long-range connections at $L > 1$ behaves like a spatial low-pass filter. The width of its bandwidth is determined by the radius of the links, and the selective properties (the ratio of transmission coefficients in the bandwidth and the barrier) — by the strength of the links γ. The connections between the mappings have an impact on their temporal and spatial dynamics. At the same time, a change in the magnitude of the coupling parameter can lead to the formation of various spatial structures in the ensemble. It's interesting to find out, to what extent do these changes correlate with the change in the shape of the wave characteristic of the coupling filter and is it possible to predict the spatial properties of the observed modes by the type of this characteristic. These questions will be considered in the course of a numerical study.

2. The system under consideration and the research algorithm

We will choose the simplest system as the object of research. It demonstrates a developed space-time chaos: a ring of N logistic maps whose equation corresponds to (1) for $F(x) = \alpha x(1-x)$, where α — a parameter that controls the dynamics of a single display.

Logistic mapping is a basic system of nonlinear dynamics. Its behavior is well known: with the growth of α it demonstrates a cascade of doubling bifurcations of periodic orbits, which ends with a transition to chaos; in the supercritical region, the development of chaotic dynamics is observed through a cascade of inverse doubling bifurcations. At $3.68 \leqslant \alpha < 4$,

the developed chaos mode is implemented in the mapping, which for weak connections ($\gamma \simeq 0$) is preserved even when combining the mappings into an ensemble. In this case, the ensemble implements a regime of homogeneous space-time chaos. In an ensemble with local connections in the range $0 < \gamma \leqslant 1$, a variety of space-time modes are observed, including dissipative structures [26].

The study of the system (1) is carried out by numerical experiment with a fixed $\alpha = 3.98$ and changing values γ and L. In the course of a numerical experiment, the limiting trajectory is determined under random initial conditions uniformly distributed in the range $]0 : 1[$, by which phase portraits and spatial images of oscillations are constructed, the mutual coherence function and spatial amplitude spectra are calculated

$$Sp\left(\bar{\omega}_k = \frac{2\pi k}{N}\right) = \sqrt{\langle X_k(n) X_k^*(n)\rangle}, \tag{6}$$

where $X_k(n) = \sum_{i=1}^{N} x_i(n) \exp(-j2\pi ki/N)$ — discrete Fourier transform (DFT) of the spatial image of oscillations at time n, k — the number of the spatial harmonic.

3. Influence of connections on mutual coherence of oscillations

With zero coupling, each of the ensemble mappings (2) demonstrates independent dynamics. Therefore, fluctuations in different cells of the network are incoherent.Coherence here refers to the mutual capture of phases in the oscillation spectra of subsystems., and the ensemble as a whole demonstrates a regime of homogeneous space-time chaos. However, as the connection grows, the fluctuations synchronize. As a result, different types of spatial and temporal behavior can be realized in the ensemble.

Let's consider how the coherence of oscillations in an ensemble changes with increasing connections for different L. To measure it, we will use the formula obtained in [23]:

$$S_{i,j} = \frac{\int_0^\infty C_{i,j}(\omega)\,(P_i(\omega) + P_j(\omega))\,d\omega}{\int_0^\infty (P_i(\omega) + P_j(\omega))\,d\omega}. \tag{7}$$

Here $C_{i,j}(\omega)$ — the mutual coherence function between the dynamics of the ith and jth mappings, P_i and P_j — corresponding power spectra. The value $S_{i,j}$ is an integral measure of the coherence of oscillations over all frequencies. It determines the ratio of the power of the coherent part of the signals of the subsystems i and j to their total power. It is a dimensionless quantity that takes values from zero (for completely incoherent signals) to one (for completely coherent ones).

In this study, we consider the coherence between neighboring oscillators $S_{i,i+1}$. In the future we will denote it as $S(i)$. Will it be the same in different parts of the ensemble or will it change from point to point? Studies show that both cases can be observed. The corresponding examples are shown in Fig. 2, where $S(i)$ graphs are plotted for two values of the local communication parameter: $\gamma = 0.16$ and $\gamma = 0.22$. As can be seen from the first graph, clusters with both high and low can coexist in the ensemble the level of coherence. To assess the coherence of the ensemble's

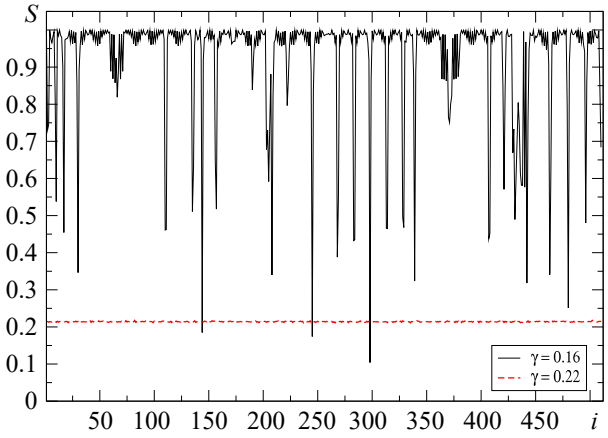

Fig. 2. Plots $S(i)$ for an ensemble with local couplings at $\gamma = 0.16$ and $\gamma = 0.22$

oscillations as a whole, it is advisable to take the average: $S_{\text{mean}} = \langle S(i) \rangle$. To estimate the heterogeneity in the distribution — maximum and minimum values: $S_{\max} = \max\{S(i)\}$, $S_{\min} = \min\{S(i)\}$. In the case of an inhomogeneous coherence distribution , the relation $S_{\min} \ll S_{\text{mean}} \ll S_{\max}$ will be executed. The opposite case is realized when $\gamma = 0.22$ (the dashed line in Fig. 2). Here $S(i)$ is practically a constant, and therefore $S_{\text{mean}} \simeq S_{\max} \simeq S_{\min}$.

Consider how S_{mean}, $S_{\max}$ and $S_{\min}$ change with the growth of γ. The calculation results are shown in Fig. 3, *a* ($L = 1$), fig. 3, *b* ($L = 2$), fig. 3, *c* ($L = 5$) and fig. 3, *d* ($L = 10$). For all the cases considered, the dependence of coherence on communication can be divided into two characteristic zones: the region of homogeneous coherence (I and III) and the region of heterogeneous coherence (II). Inhomogeneous coherence means that the ensemble contains intervals with both high ($S(i) \simeq S_{\max}$) and low ($S(i) \simeq S_{\min}$) coherence. Thus stationary spatial structures are formed (in nonlinear dynamics they are commonly called *dissipative structures*). The zone of dissipative structures is located in a narrow range of values of the coupling parameter at $\gamma \gtrsim 0.1$ and its width increases slightly with the growth of L. The uniformity zone occupies the remaining ranges of γ values: the region of weak bonds (zone I), in which coherence is close to zero, and the region of medium and strong bonds (zone III), in which coherence takes on significant values and can reach one. The latter is characterized by two typical dependencies $S_{\text{mean}}(\gamma)$: monotonous growth at $L > 1$ and unimodal character: first growth, and then fall at $L = 1$. The different behavior of the function $S_{\text{mean}}(\gamma)$ indicates a qualitative difference in

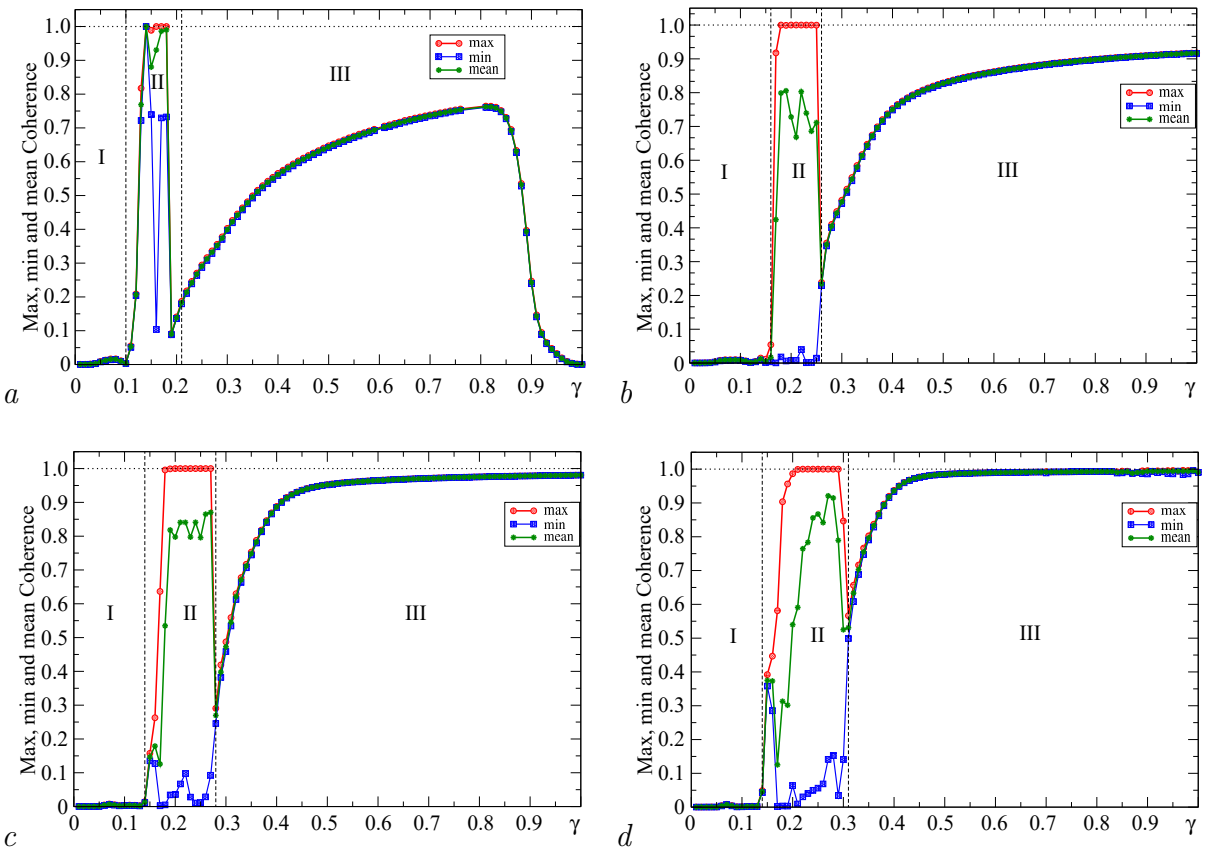

Fig. 3. Plots of coherence dependence on γ at different radii: $L = 1$ (*a*), 2 (*b*), 5 (*c*) and 10 (*d*)

the behavior of ensembles with local and non-local interaction, which is observed with strong coupling. Let's consider the behavior of the system (1) in different zones in more detail and compare it with the change in the frequency response of the link filter (3).

4. The zone of spatially homogeneous oscillations

Let us first consider the region of the coupling parameter in which coherence does not depend on the coordinate, that is, the intervals I and III. The uniformity of $S(i)$ is a consequence of the spatial uniformity of the oscillations, that is, the absence of stationary spatial structures.

Interval I. With a small connection, the selective properties of the network, which are determined by the formula (3), expressed weakly. The spatial filter is all-wave. Therefore, the spatial distribution must contain modes of all wavelengths and the resulting mode will be a developed space-time chaos. The calculations carried out confirm these assumptions. The temporal dynamics of the ensemble (2) in region I corresponds to a unicellular chaotic attractor. Spatial dynamics is a homogeneous spatial chaos. Typical phase portraits and spatial images for the mode in this area are shown in Fig. 4, *a* (for $L = 2$) and fig. 4, *b* (for $L = 10$). Similar portraits exist for other values of L. Visually, they are almost indistinguishable. However, the calculation of spatial spectra shows that there are quantitative differences between them. Consider the graphs of $Sp(\bar{\omega})$, which are shown in Fig. 5, *a*. With growth L the proportion of short-wave modes in spatial chaos decreases. The similarity of the shape of the spatial spectra with the shape of

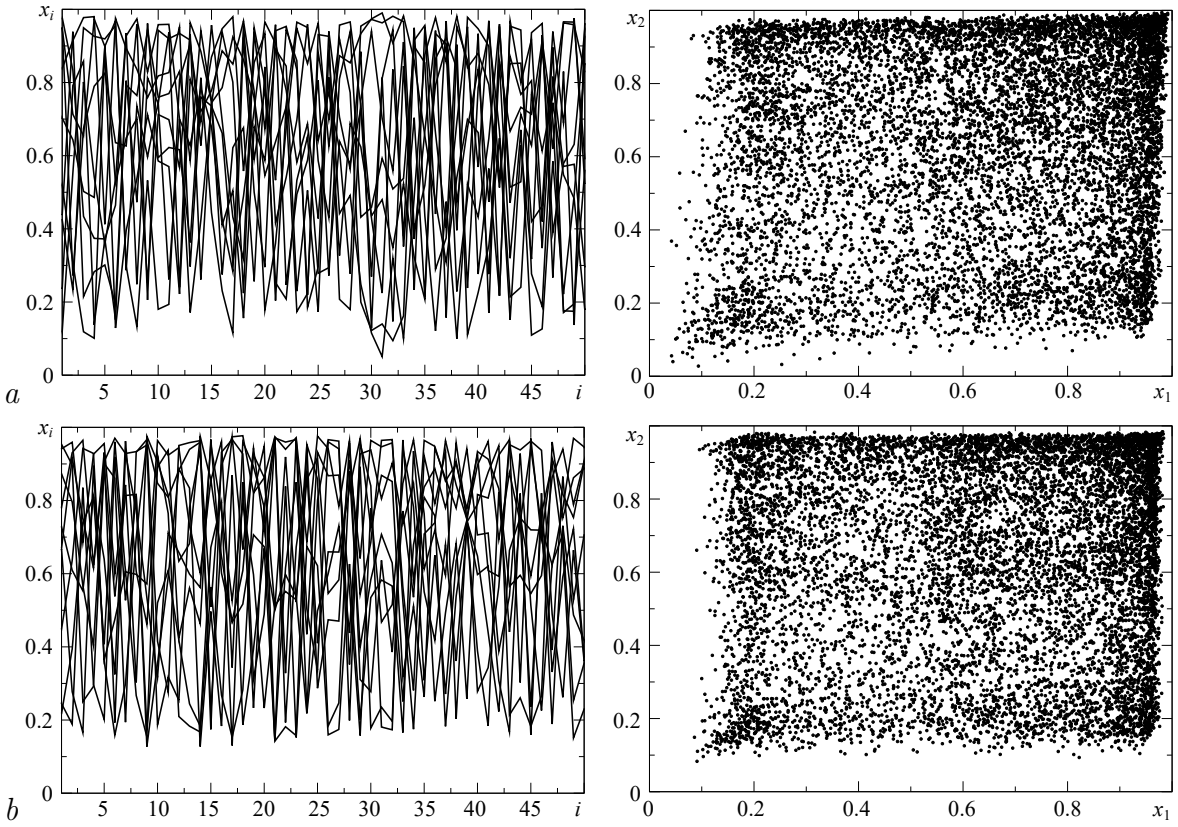

Fig. 4. System dynamics in region I: spatial snapshots (left) and cross phase-portraits (right) at $\gamma = 0.08$ and $L = 2$ (*a*), 10 (*b*)

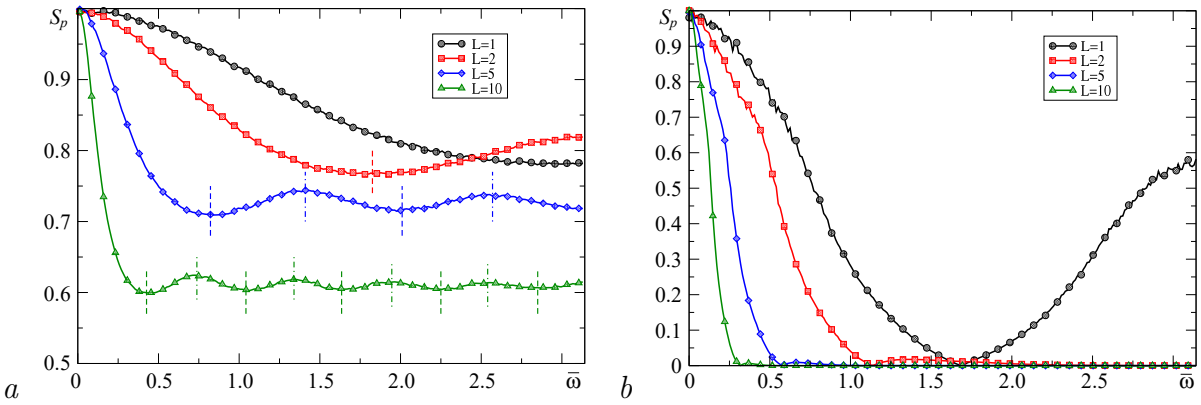

Fig. 5. Spatial spectra (a) in zone I at $\gamma = 0.08$ and (b) in zone III at $\gamma = 0.9$; on figure (a) vertical dashed and dashed-dotted lines mark minima and maxima of the frequency response plot, correspondently

the frequency response is noticeable (3): they have a similar frequency response lobe structure; moreover, the number and location of the extremes are identical (for clarity, the location of the extremes of the corresponding frequency response is marked with vertical lines). At the same time, there are quantitative differences between them: the level of the side lobes of the spectra is significantly lower than it follows from the frequency response form. The selective properties in the ensemble (2) are more pronounced than in the corresponding linear filter (**??**).

Interval III. In the region of strong coupling, there is a qualitative discrepancy in the behavior of ensembles with local and non-local connections: at $L > 1$, a monotonous increase in coherence is observed with an increase in γ (see Fig. 3, *b*, *c* and *d*), with $L = 1$ coherence initially increases, and then at $\gamma \geqslant 0.8$ begins to decrease; at $\gamma \simeq 1$ it becomes close to zero (see Fig. 3, *a*). This discrepancy is explained by the qualitative difference in the frequency response of filters. As already noted in the section 1, while non-local the connections retain the properties of the LPF in the entire range of values of γ, the system of local connections at $\gamma > 0.5$ begins to acquire the properties of a barrier filter. This is reflected in the behavior of the ensemble. As shown in [25], starting with $\gamma = 0.5$ reduction the share of short-wave modes is replaced by their growth with a maximum in the vicinity of $\bar{\omega} = \pi$. This process is dramatically enhanced at $\gamma \geqslant 0.8$. Therefore, with strong local coupling, short-wave modes are present in the spatial spectrum along with long-wave modes. Spatial dynamics is the coexistence of metastable clusters of "long" and "short" modes, as shown in Fig. 6, *a*. The intermittency between these clusters is the reason for the weakening of coherence.

A different behavior is typical for ensembles with non-local connections. Here the low-frequency character of the spatial filter is preserved even with strong coupling (see Fig. 1, *b*). Therefore, the growth of the coupling leads to a further decrease in the proportion of short-wave modes in the ensemble. This can be clearly seen from the spatial images of the oscillations plotted in Fig. 6, *b* for $L = 2$ and especially in Fig. 6, *c* for $L = 10$. As a result, with strong long-range communication, the ensemble gradually switches to a mode that is close to chaotic synchronization. This can be seen from the cross-phase portraits (see Fig. 6, *c*).

As in zone I, in the region of strong coherence, there is a qualitative coincidence between the spatial spectra of oscillations (Fig. 5, *b*) and the frequency response form (see Fig. 1, *b*). As can be seen from the figures, only long-wave components are present in all spectra except $L = 1$. However, as with weak coupling, the selective properties of the ensemble are much more

pronounced than the connections of the corresponding linear filter. Value the side lobes become so small that only those components that correspond to the main lobe remain in the spectra.

Thus, in regions I and III, the dynamics of the system (1) is a space-time chaos, the shape of the spatial spectrum of which is qualitatively similar to the amplitude-frequency response of the coupling system ($|R(\bar{\omega})|$), but does not repeat it.

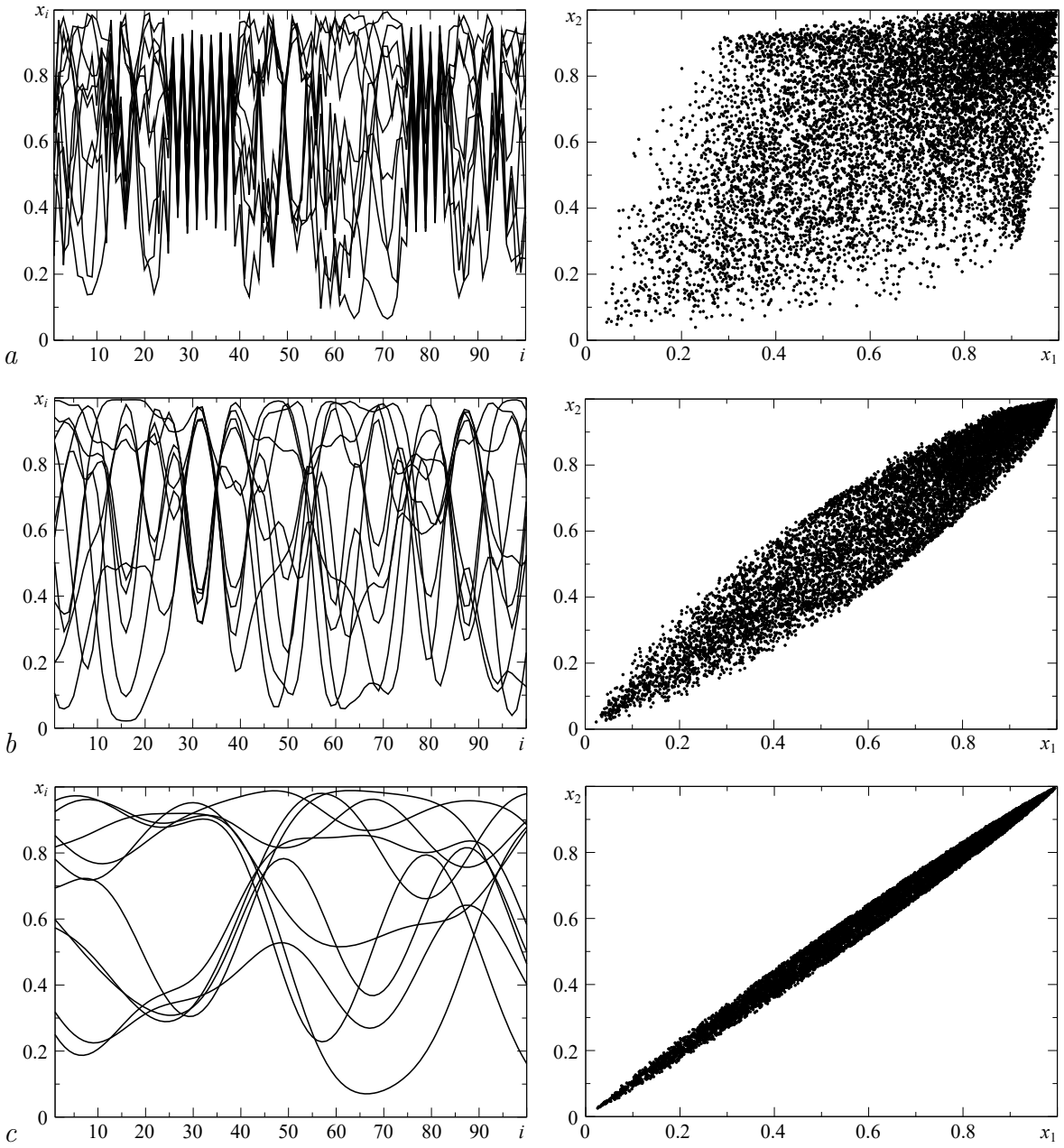

Fig. 6. The system dynamics in region III: spatial snapshots (left) and cross phase-portraits (right) at $\gamma = 0.9$ and $L = 1$ (a), 2 (b), 10 (c)

5. Zone of dissipative structures

As noted above, in most of the range $\gamma \in [0:1]$, the oscillations in the ensemble (1) represent a homogeneous space-time chaos. Let us now consider the dynamics in the remaining range of values of γ, indicated in Fig. 3 as zone II. In this area, the coherence varies along the ensemble. Both sites with full ($S(i) = 1$) and weak ($S(i)l1$) coherence coexist in it. Such heterogeneity presupposes the existence of stationary spatial structures. What is the type of these structures and will they be somehow related to the transmission coefficient of the filter R?

To answer these questions, consider typical spatial images of oscillations in the ensemble at different L, which are shown in Fig. 7. As can be seen from the figures, the resulting structures are irregular combinations of clusters with different characteristic scales, which correspond mainly to short-wave modes. So, in the case of local connections, the main mode is antiphase oscillations. Their spatial spectrum is a δ pulse at the frequency $\bar{\omega} = \pi$. At $\gamma = 0.14$, antiphase oscillations extend to the entire ensemble. In the rest of interval II, they are interspersed with short clusters of a different structure. This is shown in Fig. 7, *a*. With long-range connections, the set of alternating clusters is more diverse. But even in these cases, a high proportion of short-wave modes is obvious.

Oscillatory modes, which are shown in Fig. 7, not the only ones for these parameter values. Due to the translational symmetry of the system (1), any spatial structures that are obtained

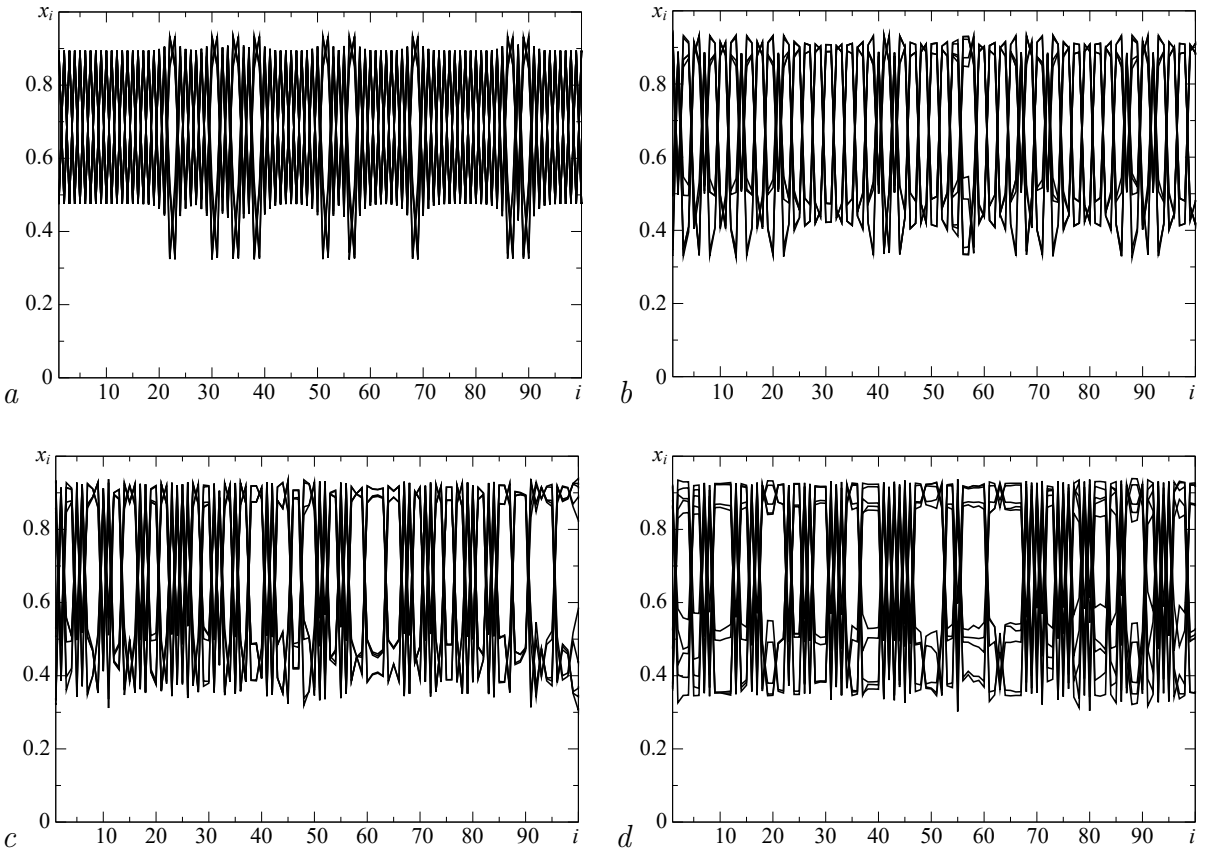

Fig. 7. The spatial snapshots in zone II at: $L = 1$, $\gamma = 0.16$ (a); $L = 2$, $\gamma = 0.18$(b); $L = 5$, $\gamma = 0.2$ (c) $L = 10$, $\gamma = 0.2$ (d)

from the images by shifting an arbitrary number of cells to the right or left will also coexist in the ensemble. In addition, there are many other similar structures. Thus, in zone II, a developed multistability is observed in the system.

To determine the quantitative composition of the wave modes that are present in the ensemble, we turn to the spatial spectra of the considered oscillatory modes. Each of the attractors will have its own spectrum, which will characterize the spatial properties of this mode. In order to characterize the system as a whole, when calculating the spectra by the formula (6) we will carry out averaging not only in time (as for spatially homogeneous modes), but also by initial conditions. The spectra constructed in this way are shown in Fig. 8.

From the analysis of the spectra, one can notice a «dip» at zero frequency, which means the suppression of long-wave modes characteristic of this zone. The spectra have a petal structure, similar to that in zone I. However, here this structure has a dual character with respect to the shape of the frequency response of the spatial coupling filter: it is easy to make sure that the maxima in the spectra correspond to the minima of the characteristic and vice versa. For greater clarity, see Fig. 8 vertical dashed lines are constructed that mark the positions of the minima of the function $R(\bar{\omega})$ for different L. The duality of the spectrum with respect to the frequency response is especially noticeable on the example of an ensemble with local connections, where the maximum is strictly at the spatial frequency $\bar{\omega} = \pi$, but it also manifests itself for long-range connections.

Thus, both in the zone of dissipative structures and in the zone of homogeneous space-time chaos, the selection of spatial modes by a network filter is observed. However, this selection occurs in the opposite way. In regions I and III, the spatial oscillation spectra turn out to be qualitatively similar to the frequency response of the coupling filter. With the growth of γ, short-wave modes are suppressed (except for the case of local connections). In zone II, mainly long-wave modes are suppressed, and the wavelengths that correspond to the frequency response minima are preserved.

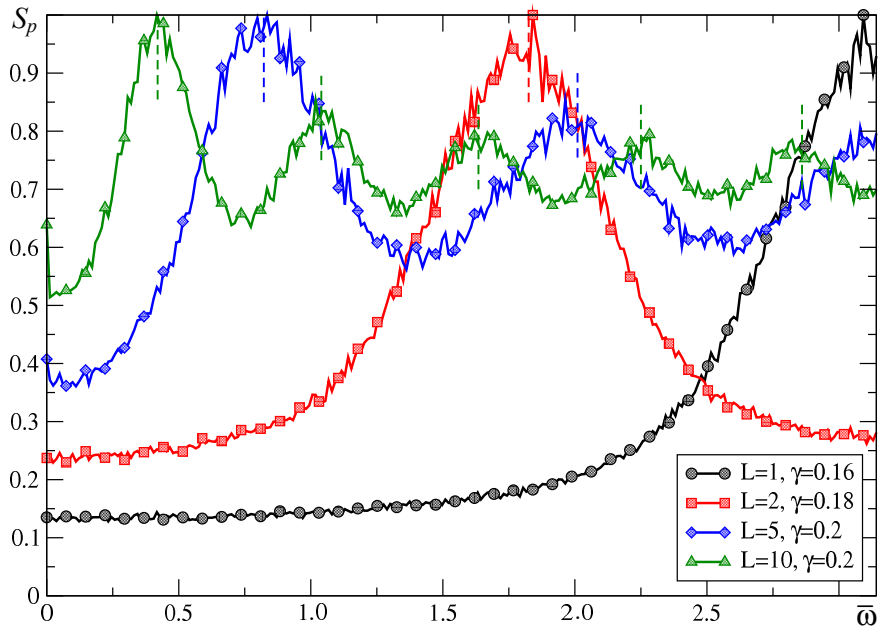

Fig. 8. Spatial spectra in the zone of dissipative structures

Conclusion

The conducted studies have shown that the system of connections between chaotic maps is a linear wave filter that has spatially selective properties. It allows spatial modes with certain wavelengths to exist and suppresses others. The selection of spatial structures is based on the wave characteristic of the link filter. Its appearance is determined by the radius of action and the magnitude of the connections between the elements of the ensemble. Selective properties are clearly manifested in the mode of developed space-time chaos. In this case , the spatial the oscillation spectrum corresponds qualitatively to the wave characteristic of the coupling filter. There is also a quantitative correspondence between the spectrum and the shape of the wave characteristic. The location of minima and maxima in the spatial spectra falls on the same wavelengths as the corresponding extremes of the wave characteristic. Nevertheless, there is no complete correspondence between them. Selective properties in a nonlinear system are significantly stronger than in the corresponding linear coupling filter.

In the course of numerical modeling of an ensemble of logistic maps It turned out that there is a characteristic qualitative difference between the dynamics of ensembles with local and non -local connections. It manifests itself in the area of strong communication. In this case, the increase in the strength of non-local connections leads to the suppression of short waves and a gradual transition to full synchronization mode. The growth of local connections leads to spatio-temporal intermittency between long-wave and short-wave clusters. At the same time, the transition to synchronization does not occur.

In addition to homogeneous space-time chaos in a small dissipative structures are observed in the coupling interval in the ensemble. The selective properties of the network are also manifested here, but “in the opposite direction”. The maxima in the characteristic of the coupling filter correspond to the minima in the distribution of the oscillation energy over the wavelengths. Therefore, in the field of dissipative structures, modes with a small wavelength become dominant.

References

1. Anishchenko VS, Postnov DE, Safonova MA. Dimension and physical properties of chaotic attractors in a chain of coupled oscillators. Sov. Tech. Phys. Lett. 1985;11(12):621.
2. Anishchenko VS, Aranson IS, Postnov DE, Rabinovich MI. Spatial synchronization and development bifurcations in a chain of coupled oscillators. Soviet Physics. Doklady. 1986;31(2):169.
3. Fujisaka H, Yamada T. Stability theory of synchronized motion in coupled-oscillator systems. Progress of Theoretical Physics. 1983;69(1):32–47. DOI: 10.1143/PTP.69.32.
4. Yamada T, Fujisaka H. Stability theory of synchronized motion in coupled-oscillator systems. II: The mapping approach. Progress of Theoretical Physics. 1983;70(5):1240–1248. DOI: 10.1143/PTP.70.1240.
5. Anishchenko VS, Vadivasova TE, Postnov DE, Safonova MA. Synchronization of chaos. International Journal of Bifurcation and Chaos. 1992;2(3):633–644. DOI: 10.1142/S0218127492000756.
6. Heagy JF, Carroll TL, Pecora LM. Synchronous chaos in coupled oscillator systems. Phys. Rev. E. 1994;50(3):1874–1884. DOI: 10.1103/PhysRevE.50.1874.
7. Ren L, Ermentrout B. Phase locking in chains of multiple-coupled oscillators. Physica D. 2000;143(1–4):56–73. DOI: 10.1016/S0167-2789(00)00096-8.
8. Shabunin AV, Akopov AA, Astakhov VV, Vadivasova TE. Running waves in a discrete anharmonic self-oscillating medium. Izvestiya VUZ. Applied Nonlinear Dynamics. 2005;13(4):37–55

(in Russian). DOI: 10.18500/0869-6632-2005-13-4-37-55.
9. Kuramoto Y. Chemical Oscillations, Waves, and Turbulence. Berlin: Springer; 1984. 158 p. DOI: 10.1007/978-3-642-69689-3.
10. Cross MC, Hohenberg PC. Pattern formation outside of equilibrium. Rev. Mod. Phys. 1993;65(3):
851–1112. DOI: 10.1103/RevModPhys.65.851.
11. Mosekilde E, Maistrenko Y, Postnov D. Chaotic Synchronization: Applications to Living Systems. Singapore: World Scientific; 2002. 440 p. DOI: 10.1142/4845.
12. Arecchi FT, Meucci R, Puccioni G, Tredicce J. Experimental evidence of subharmonic bifurcations, multistability, and turbulence in a Q-switched gas laser. Phys. Rev. Lett. 1982;49(17):1217–1220. DOI: 10.1103/PhysRevLett.49.1217.
13. Astakhov VV, Bezruchko BP, Gulyaev YV, Seleznev EP. Multistable states in dissipative coupled Feigenbaum's systems. Tech. Phys. Lett. 1989;15(3):60–65 (in Russian).
14. Astakvov VV, Bezruchko BP, Pudovochkin OB, Seleznev EP. Phase multistability and setting of the oscillations in nonlinear systems with period-doublings. Journal of Communications Technology and Electronics. 1993;38(2):291–295 (in Russian).
15. Prengel F, Wacker A, Schöll E. Simple model for multistability and domain formation in semiconductor superlattices. Phys. Rev. B. 1994;50(3):1705–1712. DOI: 10.1103/PhysRevB.50.1705.
16. Sun NG, Tsironis GP. Multistability of conductance in doped semiconductor superlattices. Phys. Rev. B. 1995;51(16):11221–11224. DOI: 10.1103/PhysRevB.51.11221.
17. Foss J, Longtin A, Mensour B, Milton J. Multistability and delayed recurrent loops. Phys. Rev. Lett. 1996;76(4):708–711. DOI: 10.1103/PhysRevLett.76.708.
18. Abrams DM, Strogatz SH. Chimera states for coupled oscillators. Phys. Rev. Lett. 2004;93(17):
174102. DOI: 10.1103/PhysRevLett.93.174102.
19. Omelchenko I, Maistrenko Y, Hövel P, Schöll E. Loss of coherence in dynamical networks: Spatial chaos and chimera states. Phys. Rev. Lett. 2011;106(23):234102.
DOI: 10.1103/PhysRevLett.106.234102.
20. Hagerstrom AM, Murphy TE, Roy R, Hövel P, Omelchenko I, Schöll E. Experimental observation of chimeras in coupled-map lattices. Nature Physics. 2012;8(9):658–661.
DOI: 10.1038/nphys2372.
21. Bogomolov SA, Strelkova GI, Schöll E, Anishchenko VS. Amplitude and phase chimeras in an ensemble of chaotic oscillators. Tech. Phys. Lett. 2016;42(7):765–768.
DOI: 10.1134/S1063785016070191.
22. Gopal R, Chandrasekar VK, Venkatesan A, Lakshmanan M. Observation and characterization of chimera states in coupled dynamical systems with nonlocal coupling. Phys. Rev. E. 2014;89(5): 052914. DOI: 10.1103/PhysRevE.89.052914.
23. Shabunin A, Astakhov V, Kurths J. Quantitative analysis of chaotic synchronization by means of coherence. Phys. Rev. E. 2005;72(1):016218. DOI: 10.1103/PhysRevE.72.016218.
24. Shabunin AV. Multistability of periodic orbits in ensembles of maps with long-range couplings. Izvestiya VUZ. Applied Nonlinear Dynamics. 2018;26(2):5–23 (in Russian).
DOI: 10.18500/0869-6632-2018-26-2-5-23.
25. Shabunin A. Selective properties of diffusive couplings and their influence on spatiotemporal chaos. Chaos. 2021;31(7):073132. DOI: 10.1063/5.0054510.
26. Kaneko K. Pattern dynamics in spatiotemporal chaos: Pattern selection, diffusion of defect and pattern competition intermettency. Physica D. 1989;34(1–2):1–41.

DOI: 10.1016/0167-2789(89)90227-3.